The Cerebellum (2019) 18:245–254
https://doi.org/10.1007/s12311-018-0987-5

ORIGINAL PAPER

TRIM9 and TRIM67 Are New Targets in Paraneoplastic Cerebellar Degeneration

Le Duy Do[1,2,3] · Stephanie L. Gupton[4] · Kunikazu Tanji[5] · Joubert Bastien[1,2,3] · Sabine Brugière[6] · Yohann Couté[6] · Isabelle Quadrio[7] · Veronique Rogemond[1,2,3] · Nicole Fabien[8] · Virginie Desestret[1,2,3] · Jerome Honnorat[1,2,3,9]

Published online: 22 October 2018

Abstract

To describe autoantibodies (Abs) against tripartite motif-containing (TRIM) protein 9 and 67 in two patients with paraneoplastic cerebellar degeneration (PCD) associated with lung adenocarcinoma. Abs were characterized using immunohistochemistry, Western blotting, cultures of murine cortical, and hippocampal neurons, immunoprecipitation, mass spectrometry, knockout mice for *Trim9* and *67*, and cell-based assay. Control samples included sera from 63 patients with small cell lung cancer without any paraneoplastic neurological syndrome, 36 patients with lung adenocarcinoma and PNS, CSF from 100 patients with autoimmune encephalitis, and CSF from 165 patients with neurodegenerative diseases. We found Abs targeting TRIM9 and TRIM67 at high concentration in the serum and the cerebrospinal fluid (CSF) of a 78-year-old woman and a 65-year-old man. Both developed subacute severe cerebellar ataxia. Brain magnetic resonance imaging found no abnormality and no cerebellar atrophy. Both had CSF inflammation with mild pleiocytosis and a few oligoclonal bands. We identified a pulmonary adenocarcinoma, confirming the paraneoplastic neurological syndrome in both patients. They received immunomodulatory and cancer treatments without improvement of cerebellar ataxia, even though both were in remission of their cancer (for more than 10 years in one patient). Anti-TRIM9 and anti-TRIM67 Abs were specific to these two patients. All control serum and CSF samples tested were negative for anti-TRIM9 and 67. Anti-TRIM9 and anti-TRIM67 Abs appeared to be specific biomarkers of PCD and should be added to the panel of antigens tested when this is suspected.

Keywords TRIM9 · TRIM67 · Autoantibodies · Lung cancer · Paraneoplastic cerebellar disorders

Electronic supplementary material The online version of this article (https://doi.org/10.1007/s12311-018-0987-5) contains supplementary material, which is available to authorized users.

✉ Jerome Honnorat
jerome.honnorat@chu-lyon.fr

Le Duy Do
le-duy.do@inserm.fr

Stephanie L. Gupton
stephanie_gupton@med.unc.edu

Kunikazu Tanji
kunikazutanji@hotmail.com

Joubert Bastien
bastien.joubert@chu-lyon.fr

Sabine Brugière
sabine.brugiere@cea.fr

Yohann Couté
yohann.coute@cea.fr

Isabelle Quadrio
isabelle.quadrio@chu-lyon.fr

Veronique Rogemond
veronique.rogemond@chu-lyon.fr

Nicole Fabien
nicole.fabien@chu-lyon.fr

Virginie Desestret
virginiedesestret@gmail.fr

Extended author information available on the last page of the article

Introduction

Paraneoplastic cerebellar degeneration (PCD) is a rare neurological syndrome characterized by subacute cerebellar ataxia associated with a systemic tumor [1]. Neurological symptoms frequently precede cancer detection. The diagnosis is mainly based on the identification of specific autoantibodies (Abs) in the serum and/or CSF of patients [1, 2]. The first described, and the most frequent, are anti-Yo Abs, also named anti-Purkinje cell cytoplasmic antibody-type 1 (PCA1) [3], but more than 30 other Abs have also been described in PCD (for review, see [2]). Although the role of these Abs in the pathophysiology of PCD is unclear, they represent a precious biomarker allowing prompt diagnosis. In clinical practice, many patients have clinical presentation of PCD without characterized associated Abs [4]. Herein, we describe novel Abs targeting the brain antigens tripartite motif-containing (TRIM) protein 9 (TRIM9) and 67 (TRIM67) in two patients with PCD and lung adenocarcinoma.

Materials and Methods

Patients

Between October 2007 and June 2016, we tested more than 8000 CSF samples of patients suspected of autoimmune encephalitis or paraneoplastic neurological syndrome in the French reference center. Among them, using immunohistochemistry, we identified 32 samples with Abs directed against uncharacterized neuronal targets and with clinical presentation highly suggestive of PCD. To perform future characterization, samples of these patients were deposited in the "NeuroBioTec" biobank of the Hospices Civils de Lyon (France, AC-208-73, NFS96-900). To evaluate the specificity of anti-TRIM9/TRIM67 Abs, we also tested sera from 63 patients with small cell lung cancer but without any paraneoplastic neurological syndrome, 36 patients with lung adenocarcinoma and PNS (7 with Ma2, 16 with Hu, and 13 without antibodies), CSF from 100 patients with autoimmune encephalitis (29 patients with an associated cancer, and 71 without), and CSF of 165 patients with no inflammatory neurodegenerative diseases (25 with fronto-temporal dementia, 15 Lewy body disease, 20 with psychosis, 15 with communicant hydrocephalus, and 90 with Alzheimer's disease).

Written consent was obtained from all patients, and the study was approved by the institutional review board of the University Claude Bernard Lyon 1 and Hospices Civils de Lyon. All clinical and paraclinical data of these patients were collected by study investigators and clinical research associates at the time of PCD diagnosis and during follow-up.

Mice

Mouse lines were on a C57BL/7 background and were housed and bred at the University of North Carolina with approval from the Institutional Animal Care and Use Committee. Timed pregnant females were obtained by placing male and female mice together overnight; the following day was designated as E0.5 if the female had a vaginal plug. *Trim9*$^{-/-}$ mice and *Trim67*$^{-/-}$ mice have been previously described [5, 6]. *Trim9*$^{-/-}$:*Trim67*$^{-/-}$ mice, generated by crossing *Trim9*$^{-/-}$ mice and *Trim67*$^{-/-}$ mice, were viable and will be described in more detail below.

Immunohistochemistry

Freshly prepared adult rat and mouse brains were fixed in 4% paraformaldehyde (PFA) for 1 h, frozen, and sliced into 10-μm-thick sections. Immunolabeling was performed using patient CSF (1:10) and revealed with peroxidase-conjugated secondary antibody against human IgGs (1:1000, 709-065-149 J, Jackson Immunoresearch, Immunotech, Montluçon, France). For fluorescent labeling, immunostaining was revealed with appropriate Alexa fluorophore-conjugated secondary antibodies (1:1500, A11013, Thermofisher, Courtaboeuf, France).

Western Blot

Whole adult rat brains were dislocated. The tissue was homogenated in lysis buffer containing 50 mM Tris-HCl pH 7.5, 150 mM NaCl, 1 mM EDTA, 1% NP-40, 0.5% deoxycholate, 0.1% SDS, orthovanadate, benzonase, phosphatase inhibitor, and protease inhibitor. The homogenate was incubated on ice for 30 min then sonicated. Cell debris was discarded by 10 min centrifugation at 10000*g* and 4 °C. Twenty micrograms of whole brain protein extract was used for Western blotting to screen specific band recognized by patient CSF (1/100).

Immunoprecipitation and Mass Spectrometry-Based Identification

A positive CSF (patient 1) and a negative CSF (control CSF) were used. Five microliters of CSF was mixed with 50 μL of protein G-conjugated agarose beads (Sigma-Aldrich, Lyon, France) and completed to 500 μL with PBS. The mixture was incubated for 2 h at 4 °C with rotation to allow for coupling of CSF antibodies to protein G. Simultaneously, whole protein extract from one mouse brain was prepared and incubated with 50 μL of agarose beads. Nonspecific contaminant was removed from the lysate by 5 min centrifugation at 16000*g* and 4 °C. Cleared lysate was subsequently used for immunoprecipitation with antibody-conjugated agarose

beads. Immunoprecipitate was analyzed by SDS-PAGE, and this was followed by silver-stain and Western blotting. The area between 72 and 95 kDa of a Coomassie-blue stained gel was excised and analyzed by mass spectrometry-based proteomics, as previously described [7]. Briefly, proteins were in-gel digested using modified trypsin (sequencing grade, Promega, Charbonnières, France), and resulting peptides were analyzed by online nanoLC-MS/MS (UltiMate 3000 and LTQ-Orbitrap Velos Pro, Thermo Scientific, Grenoble, France). Peptides and proteins from different samples were identified, filtered, and compared using Mascot and Proline software (Profi Proteomics, Toulouse, France).

Cell-Based Assay

To confirm the target of the Abs, HEK 293 cells were transfected with pCS2-*Trim9*(mouse) plasmid [8] or pCS2-*Trim67*(mouse) plasmid [6] for transient overexpression. Fixed and permeabilized cells were then immunostained using patient CSF (1:100) and commercial mouse monoclonal anti-Myc antibody (ab9106, Abcam, Paris, France) and then they were revealed with appropriate fluorochrome-conjugated secondary antibodies (1:1500, A11013, and A11001, Thermofisher, Courtaboeuf, France). Images of stained cells were taken with fluorescent microscope Axio Imager Z1 (Carl Zeiss, Marly-le-Roi, France). Antibody titers were obtained by using serial dilutions of serum and CSF, as well as full-length *TRIM9*-transfected HEK 293 cells. Patients' antibody IgG subtypes contained in serum or CSF were identified using full-length *TRIM9*-transfected HEK 293 cells and secondary anti-human antibodies specific for IgG1 (MCA4774, Bio-Rad, Hercules, CA), IgG2 (555873, BD Pharmingen, Le Pont de Claix, France), IgG3 (5247-9850, ABD serotec, Kidlington, OX), and IgG4 (555881, BD pharmingen). For epitope mapping on TRIM9, several plasmids coding for different domains were used [9]. For epitope mapping on TRIM67, we generated three constructions coding for the N-terminal region (F1), B-Box domain (F2), and C-terminal region containing Coiled-coil, FnBD, and B30.2 domains (F3), using PCR (In fusion, Clontech, Mountain View, CA) and primers as indicated in Table 1.

Effects of Patient CSF on Neuronal Viability and Development

Embryonic day (E) 15.5 cortical neurons were dissociated from wildtype (+/+) and *Trim9*$^{-/-}$:*Trim67*$^{-/-}$ (double KO) mice and cultured on Poly-D-Lysine (Sigma-Aldrich) coated coverslips for 96 h in Neurobasal media supplemented with glutamine and b27 (Invitrogen, Carlsbad, CA) prior to fixation in 4% PFA in PHEM buffer. Neurons were left untreated, or incubated with patient CSF (1:100) for either 1 or 3 days prior to fixation. Neurons were stained for filamentous actin (phalloidin), βIII tubulin (neuronal marker), and nuclei (DAPI). Neurons were imaged by widefield epifluorescence with a × 20, 1.3 NA PlanApo objective on an inverted Olympus IX-81ZDC microscope with an iXon 1K EM-CCD camera (Oxford Instruments, Concord, MA). Viable and non-viable cells were counted as spread nuclei with visible nucleoli and contracted nuclei without visible nuclei, respectively; differences were tested using an ANOVA with no post hoc correction. Neurites were measured using the NeuronJ plugin in ImageJ. The longest neurite was considered the axon. Several parameters were measured per neuron, including density of axon branches, primary axon length, total axonal material (summed length of all axon and branches), dendritic material (summed length of all dendrites and branches), primary dendrite number, and dendrite branch points. ANOVA with Bonferroni post hoc correction was performed to compare treatments to untreated control and to compare the two genotypes in the untreated condition. Corrected p values are shown for significant differences. For all tests, $p < 0.05$ was considered significant.

Table 1 List of primers used for cloning of different domains of TRIM67

F1	F2	F3
FW: GGCGGTGT AGCCTG GTGGCT CCCGC	FW1: ATTCAATG GCCATCTGCCAG CTGTGC	FW: ATTCAATG AAAGAG AGGGAG CACAAGC
RV: CAGGCTAC ACCGCC GGGGCT GCAGC	RV1: AGATGGCC ATTGAATTCAAG TCCTCTTCAGAA	RV: TCTCTTTC ATTGAATTCAAG TCCTCTTCAGA
	FW2: AGGTGACC TAGCCTGGTGGC TCCCGC	
	RV2: CAGGCTAG GTCACCTTGGTG AGCAGC	

FW, forward primer; *RV*, reverse primer. For F2 cloning, we performed two successive PCRs using respectively FW1, RV1 and FW2, RV2 primers for each step

Results

TRIM9 and TRIM67 Are Targeted by CSF Autoantibodies of Two Patients with PCD

Among the 32 samples of patients with suspected PCD and Abs directed against uncharacterized neuronal targets, the CSF of patient 1 was identified as having particular reactivity with the cytoplasm of neurons and neuropil of the cerebellum, hippocampus, and cerebral cortex that was distinct from known Abs associated with PCD (Fig. 1a, upper panels). Indirect immunohistochemistry on rat brain section found diffuse immunoreactivity in the cytoplasm of the soma and

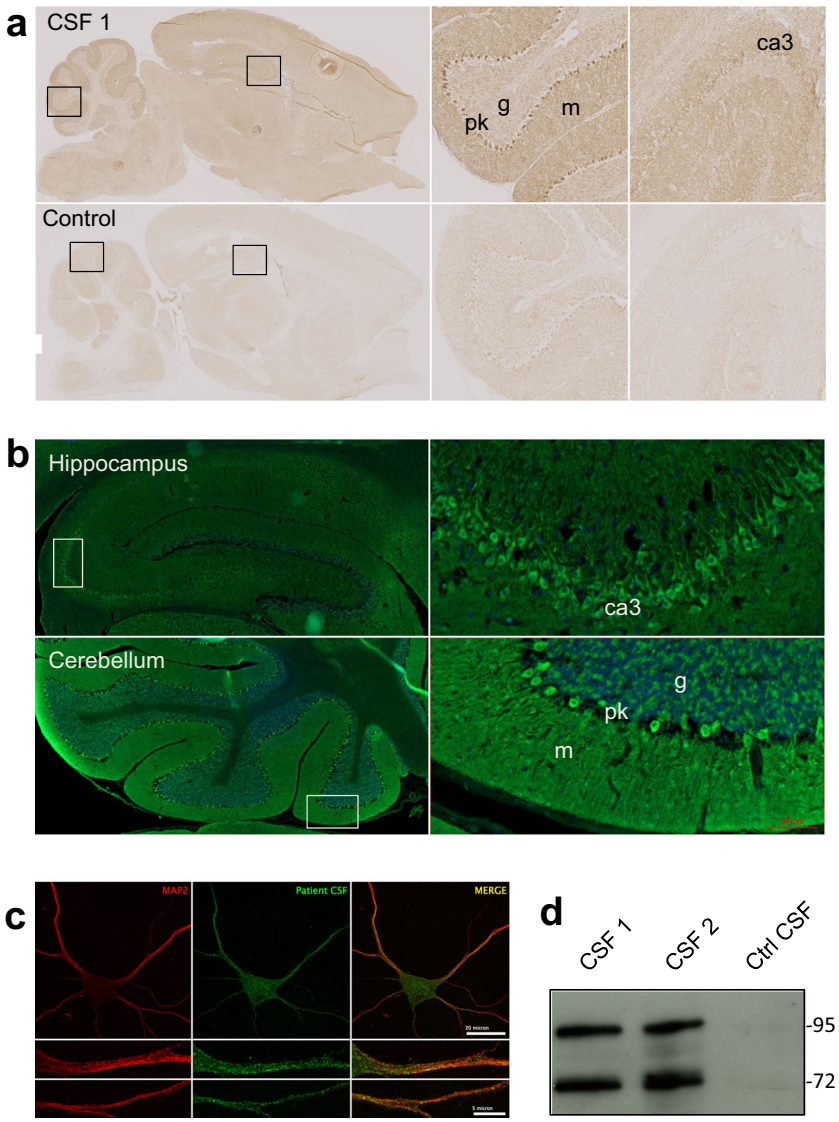

Fig. 1 **a** Immunohistochemistry of adult rat brain with cerebrospinal fluid (CSF) from patient 1 (upper panels) or control CSF (lower panels). Note a strong staining of CA3 pyramidal cells in the hippocampus and the granular layer and Purkinje cell layer in the cerebellum. **b** Fluorescent staining of rat brain with CSF from patient 1. Note a strong reactivity with the cell bodies and proximal dendrite of the pyramidal cells in the hippocampus (upper panels) and those of Purkinje cell in the cerebellum (lower panel). **c** Immunolabeling of embryonic hippocampal neurons (at div15) with CSF from patient 1. Abs in the CSF recognized cytosolic proteins organized in small speckles in the cell bodies and dendrites. **d** Western blotting showing reactivity of patient CSF. Targeted proteins were enriched by immunoprecipitation using CSF from patient 1. Bands at 72 and 95 kDa were excised and analyzed by mass spectrometry. m molecular layer, g granular layer, pk Purkinje cell layer

proximal dendrite of CA3 neurons in the hippocampus (Fig. 1b, upper panels). In the cerebellum, marked immunolabeling was observed in neuropil of the molecular layer, in cell bodies and dendrites of Purkinje cells, and to a less extent in the cytoplasm of granule cells (Fig. 1b, lower panels). Immunostaining of fixed and permeabilized murine neurons found labeling of cytosolic clusters (Fig. 1c). However, no labeling was observed on live neurons, suggesting that the Abs exclusively targeted intracellular proteins.

Western-blots using rodent brain protein extract showed that CSF from patient 1 recognized two specific protein bands at ~ 72 and ~ 95 kDa (Fig. 1d). To identify the antigen, whole mouse brain homogenate was incubated with CSF from patient 1, and the antigen was immunoprecipitated. Subsequent mass spectrometry analyses found that TRIM9 and TRIM67 were specifically enriched in the 95-kDa band and that the 72-kDa band also contained TRIM9, but not TRIM67.

To confirm the presence of anti-TRIM9 and TRIM67-Abs in CSF from patient 1, HEK293 cells were transfected with full-length cMyc-tagged TRIM9 or TRIM67 plasmids. The CSF recognized both TRIM9- and TRIM67-expressing cells, demonstrating that the CSF contained Abs recognizing the two proteins; control CSF did not (Fig. 2a). No staining was observed on double KO mice brain slices (Fig. 2b), indicating that the Abs in the CSF from patient 1 were only raised against TRIM9 and TRIM67. Immunostaining on *Trim9*$^{-/-}$ single KO mouse brain found expression of TRIM67, and on *Trim67*$^{-/-}$ mouse brain found expression of TRIM9 (Fig. 2b); TRIM9 was widely expressed, notably in the hippocampus, and TRIM67 in the cerebellum, as previously described [6].

The 31 other patients with suspected PCD were screened using the HEK293 transfected cells and a second patient with anti-TRIM9 and anti-TRIM67-Abs in her CSF (patient 2; Supplemental fig. S1).

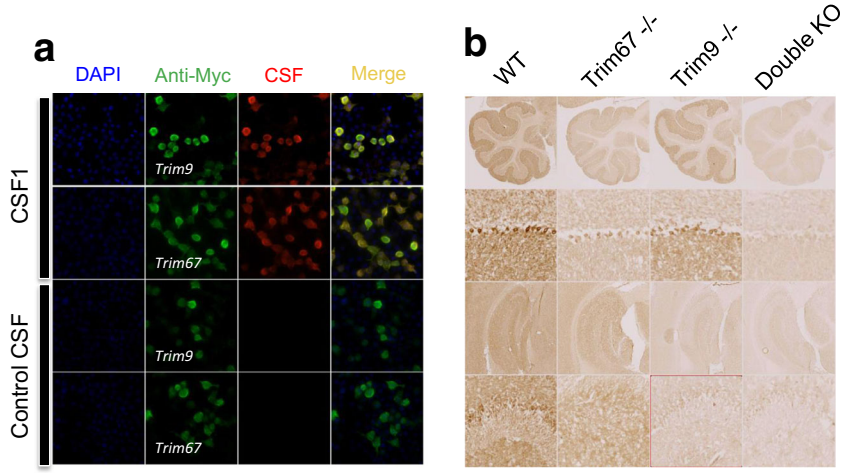

Fig. 2 **a** Cell-based assay test to confirm the identity of Abs targets. HEK cells were transfected with plasmids coding for Myc-tagged TRIM9 or Myc-tagged TRIM67 for transient overexpression. Transfected cells were fixed, permeabilized, and immunolabeled with patient CSF (red) or commercial anti-Myc antibody (green). Colocalization of the two stains confirmed that Abs recognized TRIM9 and TRIM67. **b** Immunostaining of single or double knockout (KO) mouse brain with CSF from patient 1. TRIM9 was expressed widely in the adult brain while TRIM67 is more restricted to the cerebellum

Clinical Presentation of Patients 1 and 2

Patient 1

A 78-year-old woman, with past medical history characterized by 30 pack-years of cigarettes and type II diabetes mellitus treated by diet. She developed subacutely (within less than 1 month) severe cerebellar ataxia. The patient was unable to walk without support. Examination found dysarthria, a severe static cerebellar syndrome with extension of the support polygon, and an inability to stand up without help. Dysmetria and hypermetria were severe in the inferior limbs. No motor or sensory deficit was observed, but she had cognitive impairment with anterograde amnesia and dysexecutive symptoms (Mini-mental scale was 20/30 and Frontal Assessment Battery 8/18). Initial brain MRI was normal and the CSF showed inflammation (protein 0.65 g/l; lymphocytes 17/mm^3; more than 10 oligoclonal bands (OCBs); IgG index of 1.52 (normal < 0.7)). A fluorodeoxyglucose body positron-emission tomography (PET) scan found a mediastinal highly metabolic lymph node, and a biopsy found the presence of a poorly differentiated adenocarcinoma (CK7 and TTF1 positive, without EGFR, KRAS, BRAF, or ERBB2 mutation). The patient was treated by chemotherapy (carboplatine and taxol), corticosteroids, and immunoglobulins without effect on the neurological symptoms and with a partial effect on the cancer. She is still alive 2 years after disease onset.

Patient 2

A 65-year-old man, with past medical history characterized by 80 pack-years of cigarettes and pulmonary right lobar well-differentiated adenocarcinoma (stage 1B T2N0), was diagnosed 2 years before and treated by surgery only. He developed subacutely (within less than 1 month) isolated and severe cerebellar ataxia. The patient was unable to walk without support and developed dysarthria. Examination found a severe static cerebellar syndrome with extension of the support polygon and inability to stand up without help. A mild dysmetria and hypermetria were also observed, predominantly on the left side. No motor, sensory, or cognitive deficit was observed. Initial brain computed tomography scan was normal and the CSF showed inflammation (protein 0.41 g/l; lymphocytes 9/mm^3 with activated lymphoplasmocytes; few OCBs; an IgG index of 0.65 (normal < 0.7)). A fluorodeoxyglucose body PET scan showed a mediastinal highly metabolic lymph node 1.5 cm in size suggesting a metastatic evolution of the pulmonary adenocarcinoma. The patient refused further investigations, all immunomodulatory treatment and was lost of follow-up during 10 years after mediastinal radiotherapy. Twelve years later, the patient is still alive with a stable but severe cerebellar ataxia and without recurrence of his cancer.

Specificities of Patients 1 and 2 Abs

The technique of "end-point dilution" on HEK293 cells was employed to estimate Ab titers in the serum and the CSF of the two positive patients. Patient 1 had higher anti-TRIM9 Ab titer than patient 2 (serum 1/128,000, CSF 1/8000 versus 1/64000 and 1/4000, respectively), while anti-TRIM67 Ab titers in both patients were identical (serum 1/256000, CSF 1/8000).

As Abs against TRIM46, a closely related class I (I-3) member of the TRIM family, have been described in three

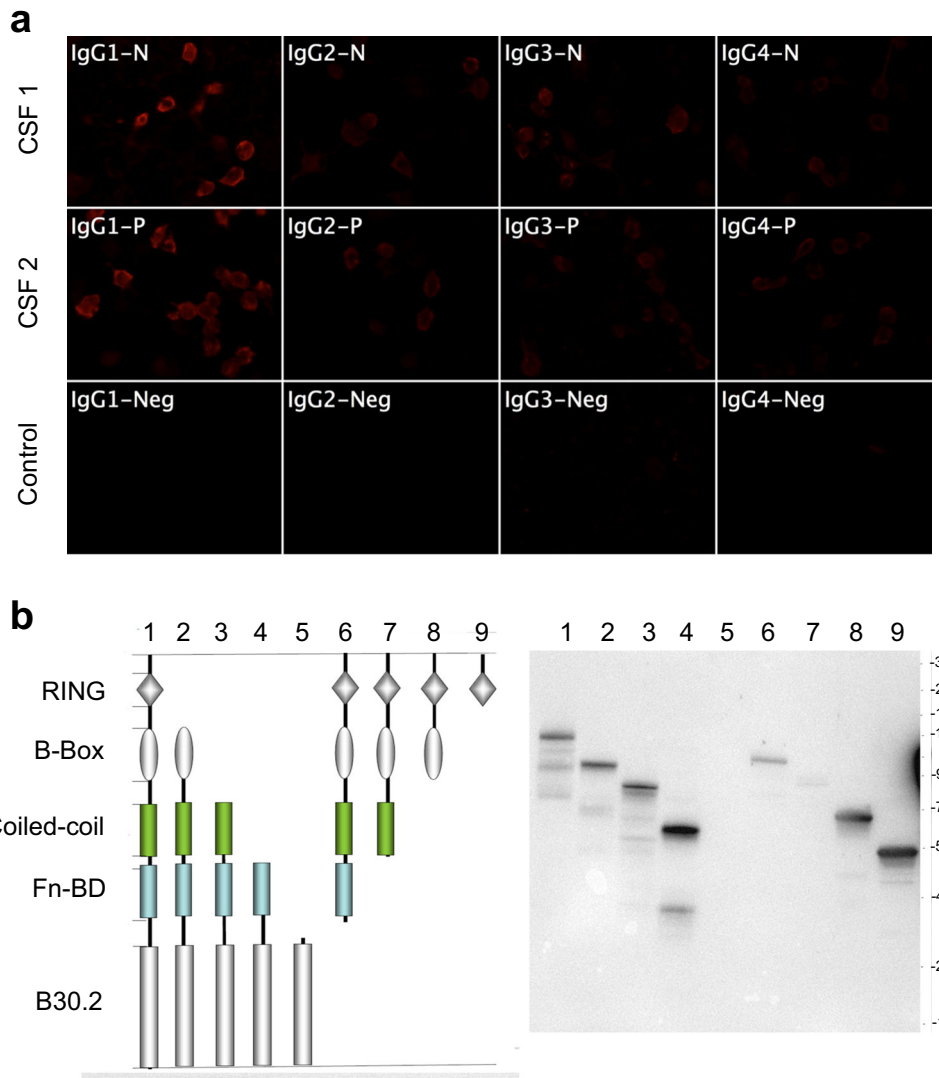

Fig. 3 **a** Analysis of the IgG subclass of anti-TRIM9 Abs in patient CSF. HEK cells expressing TRIM9 were incubated with patient CSF and revealed with subclass-specific anti-human IgG antibodies. Positive signal was observed for all IgG subclasses; the strongest signal was found for IgG1. **b** Epitope mapping of anti-TRIM9 Abs. HEK cells were transfected with plasmids coding for different domains of TRIM9 and then lysed and immuno-blotted with CSF from patient 1 that recognized all TRIM9 domains except the B30.2 domain. The Abs are polyclonal

patients having paraneoplastic neurological syndromes [10], we tested whether the Abs also recognized TRIM46; both patients were negative (Supplemental fig. S1).

To ensure that anti-TRIM9 and TRIM67-Abs were specific to PCD, we tested transfected HEK cells expressing TRIM9 or TRIM67 with sera and CSF of 364 controls; all were negative.

Characteristics of TRIM-Abs

Analysis of IgG composition found that CSF of both patients contained mainly IgG1 and that other IgG subclasses (IgG2, 3, and 4) were only very weakly positive (Fig. 3a). DNA constructs coding for different domains of TRIM9 and TRIM67 were used to probe the protein domain containing the epitope for the Abs. Results from Western blotting experiments indicated that Abs in the CSF of both patients were polyclonal, since Abs recognized at least two different epitopes on the TRIM9 protein, one in the RING domain and the other in B-Box, Coiled-coil or FnBD-3 domain, but not the B30.2 (Fig. 3b). On the TRIM67, Abs reacted strongly with the B-Box domain

Fig. 4 Effects of Patient CSF on neuronal viability and development. ▶ E15.5 cortical neurons from wildtype (+/+) and *Trim9*$^{-/-}$:*Trim67*$^{-/-}$ (double KO) mice were treated with patient CSF (1:100) for 3 days or 1 day prior to fixation. Neurons were stained for ßIII tubulin (green), filamentous actin (red), and DNA (blue). Several parameters were measured per neuron, including density of axon branches, primary axon length, total axonal material, dendritic material, primary dendrite number, and dendrite branch points. In the box and whisker plots: the cyan boxes for each genotype are untreated. The second two were incubated from the 24th to the 96th hour (3 days) with 1:100 CSF from patient 1 (magenta boxes) and patient 2 (yellow boxes), respectively; the next two were incubated from the 72nd to the 96th hour (1 day), patient 1 and patient 2, respectively. Boxplots depict median ± the interquartile range (IQR), and whiskers reach minimum and maximum values. *p* values were determined by ANOVA, comparisons made to untreated control, with Bonferroni post hoc corrections of the number of comparisons made. *p* values are considered significant when $p < 0.05$. No consistent significant effects of patients' CSF on neurons were observed

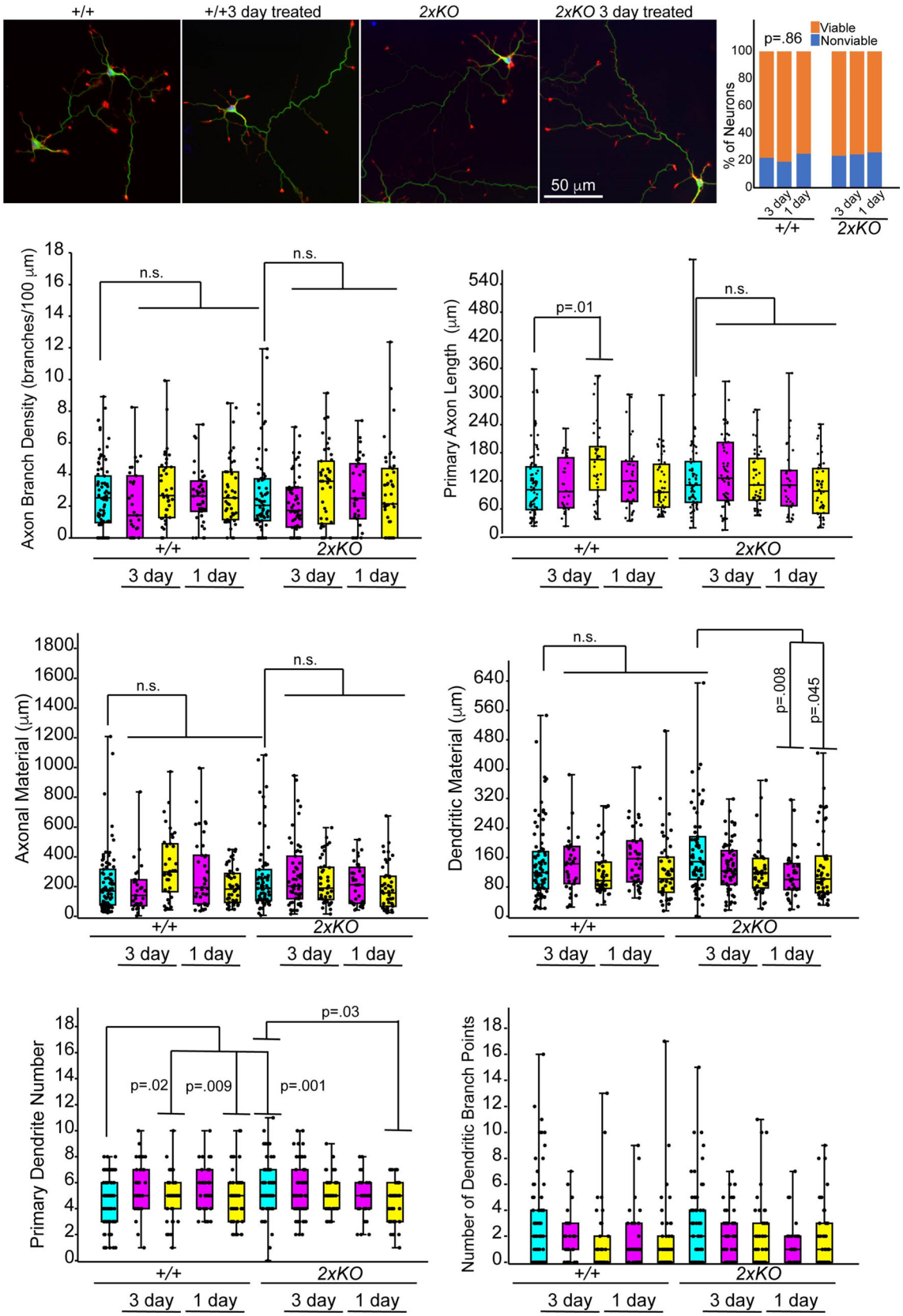

and the one in C-terminal containing Coiled-coil, FnBD-3, and B30.2 domain. Unlike TRIM9, the TRIM67 N-terminal containing RING domain was very weakly recognized by the Abs (Supplemental fig. S2).

Effect of CSF Autoantibodies on Neurons

TRIM9 and TRIM67 have both been implicated in the morphogenesis of developing neurons or neuron-like cells [5, 8, 11]. To investigate a potential pathogenic mechanism and examine whether Abs affect TRIM-dependent neuronal morphogenesis, the effect of patient CSF on developing murine cortical neurons was studied in vitro. No significant effect of antibodies on neuron viability or consistent detriment to neuronal morphogenesis was observed (Fig. 4).

Discussion

The results of the present study demonstrate that TRIM9 and TRIM67 are new targets of Abs in PCD associated with lung carcinoma. These Abs appear to be highly specific biomarkers, since they were not found in the CSF or sera of control patients. These results are reinforced by the previous identification of anti-TRIM9 and anti-TRIM67-Abs in a woman with PCD secondary to a melanoma [12], suggesting that other cancers could also be the trigger of such antibodies. Exploratory epitope mapping found that the immune reaction was polyclonal, with Abs that recognize multiple epitopes on the two proteins. These Abs are mainly of IgG1 subtype.

The TRIM protein family is a highly conserved superfamily of E3 ubiquitin ligases that include 76 members; TRIM9 and TRIM67 belong to the class I-2 [13]. Antibodies targeting TRIM21 and 46 have been described in other autoimmune diseases. For instance, the presence of anti-TRIM21 Abs (Ro52) in serum has been described in association with different immune-mediated diseases such as Sjögren's syndrome, systemic lupus erythematosus, systemic sclerosis, and autoimmune myositis (for review, see [14]). More recently, anti-TRIM46 Abs have been described in three patients with paraneoplastic neurological syndromes associated with small cell lung carcinoma [10]. Although both patients presented herein were negative for anti-TRIM46, the serum of patient 1 was found to be positive for anti-TRIM21 Abs using standard diagnostic tests (dot-blot and luminex, data not shown); the serum of patient 2 was negative. However, as no immunostaining with patient CSF was observed on the brain of *Trim9*$^{-/-}$ and *Trim67*$^{-/-}$ double KO mice, we can conclude that CSF of the two patients described herein contained only anti-TRIM9 and anti-TRIM67 Abs; positivity for anti-TRIM21-Abs positivity in the serum of patient 1 could be a consequence of a cross-reactivity.

TRIM9 is widely expressed in embryonic and adult mouse brain [15, 16]. In the latter, TRIM9 localizes in the cytoplasm and proximal dendrites of pyramidal cells in the hippocampus, the Purkinje cells of the cerebellum, and in the external layer of the cortex [9, 16]. Immunostaining of *Trim67*$^{-/-}$ mouse brain confirmed these observations. TRIM67 is abundantly expressed in the cerebellum of both mouse and human [6, 11], and immunostaining with patient CSF herein showed a similar pattern.

The two patients reported herein developed subacute severe cerebellar ataxia. Lung carcinoma was discovered and treated; however, neurological symptoms persisted which could be due to irreversible neuronal loss. In addition, patient 1, having a higher anti-TRIM9 Ab titer, developed more severe neurological impairment including cognitive impairment with anterograde amnesia and dysexecutive symptoms, which were absent in patient 2.

Although it lacks any identified membrane targeting domain, TRIM9 does interact with the membrane-associated SNARE protein, SNAP25, and acts as negative regulator of exocytosis during axonal branching and growth [5]. TRIM9 also interacts with and ubiquitinates DCC, a transmembrane receptor for netrin-1 [5, 17], and the actin polymerase VASP [8]. Upon binding of netrin-1 to its receptor DCC, TRIM9 releases SNAP25 and VASP is deubiquitinated, promoting vesicle fusion, membrane expansion, and membrane protrusion [5, 8]. In patients with dementia and Lewy bodies, TRIM9 expression in the brain is reduced [9]. Furthermore, in animal models, absence of TRIM9 causes excessive dendrite arborization, mislocalization, and decreased dendritic density in adult-born neurons of the dentate gyrus, leading to impairment of learning and memory [18]. TRIM67 interacts with TRIM9 and DCC and plays an important role in brain development and behavior, including learning and memory and cognitive flexibility [6]. These two proteins seem therefore to play a major role in neuronal function, and we therefore investigated the pathogenicity of Abs on neurons. However, we did not observe any effect of patient CSF on cortical neuron survival or growth in vitro. As immunostaining on living neurons was negative, the absence of direct interaction between Abs and the antigen is probable explaining the absence of pathogenic effect. This result is similar to other onconeural Abs targeting intracellular antigens [19, 20].

To conclude, the present study demonstrates that Abs against TRIM9 and TRIM67 are biomarkers of some rare cases of PCD and seem to be mainly associated with lung carcinoma. Anti-TRIM9 and TRIM67 Abs should be added to the routine diagnostic tests performed for patients with suspicion of PCD and negative for previously described Abs. Furthermore, efforts must be made to provide prompt diagnosis and to try early immunomodulatory treatment as cerebellar ataxia seems to be irreversible owing to neuronal death.

Acknowledgments We thank Professor Casper Hoogenraad, Faculty of Science, Utrecht University for providing us with the Trim46 plasmid construct.

Authors' contribution Dr. Le Duy DO: acquisition, analysis, and interpretation of the data; drafting the manuscript for intellectual content

Prof. Stephanie L Gupton: generated and provided *Trim9*$^{-/-}$, *Trim67*$^{-/-}$, and *Trim9*$^{-/-}$/*Trim67*$^{-/-}$ mice, experimental design, acquisition, analysis,

and interpretation of the mouse neuron data; critical revision of the manuscript for important intellectual content

Dr. Kunikazu Tanji: provided plasmids coding for different domains of TRIM9

Dr. Joubert Bastien: acquisition and analysis of data

Sabine Brugière and Dr. Yohann Couté: performed mass spectrometry and collected data

Pr. Isabelle Quadrio: provided CSF sample of control group

Dr. Véronique Rogemond: acquisition and analysis of data

Dr. Nicole Fabien: acquisition and analysis of data

Dr. Virginie Desestret: analysis and interpretation, critical revision of the manuscript for important intellectual content, study supervision

Pr Jérôme Honnorat: study concept and design, analysis and interpretation, critical revision of the manuscript for important intellectual content, study supervision

Funding Information This study was supported by research grants from the Agence Nationale de la Recherche (ANR-14-CE15-0001-MECANO), the Fondation pour la recherche médicale (DQ20170336751), and the National Institutes of Health (GM108970, S.L.G.). Proteomic experiments were partly supported by the Proteomics French Infrastructure (ANR-10-603 INBS-08-01 grant) and Labex GRAL (ANR-10-LABX-49-01).

Compliance with Ethical Standards

Conflict of Interest The authors declare that they have no conflict of interest.

References

1. Honnorat J, Cartalat-Carel S. Advances in paraneoplastic neurological syndromes. Curr Opin Oncol. 2004;16(6):614–20.
2. Jarius S, Wildemann B. 'Medusa head ataxia': the expanding spectrum of Purkinje cell antibodies in autoimmune cerebellar ataxia. J Neuroinflammation. 2015;12:166–8.
3. Greenlee JE, Brashear HR. Antibodies to cerebellar Purkinje cells in patients with paraneoplastic cerebellar degeneration and ovarian carcinoma. Ann Neurol. 1983;14(6):609–13.
4. Ducray F, Demarquay G, Graus F, Decullier E, Antoine JC, Giometto B, et al. Seronegative paraneoplastic cerebellar degeneration: the PNS Euronetwork experience. Eur J Neurol. 2014 May;21(5):731–5.
5. Winkle CC, McClain LM, Valtschanoff JG, Park CS, Maglione C, Gupton SL. A novel Netrin-1–sensitive mechanism promotes local SNARE-mediated exocytosis during axon branching. J Cell Biol. 2014;205(2):217–32.
6. Boyer NP, Monkiewicz C, Menon S, Moy SS, Gupton SL. Mammalian TRIM67 functions in brain development and behavior. eNeuro. 2018;5(3):ENEURO.0186–18.2018.
7. Casabona MG, Vandenbrouck Y, Attree I, Couté Y. Proteomic characterization of Pseudomonas aeruginosa PAO1 inner membrane. Proteomics. 2013;13:2419–23.
8. Menon S, Boyer NP, Winkle CC, McClain LM, Hanlin CC, Pandey D, et al. The E3 ubiquitin ligase TRIM9 is a filopodia off switch required for netrin-dependent axon guidance. Dev Cell. 2015;35(6):698–712.
9. Tanji K, Kamitani T, Mori F, Kakita A, Takahashi H, Wakabayashi K. TRIM9, a novel brain-specific E3 ubiquitin ligase, is repressed in the brain of Parkinson's disease and dementia with Lewy bodies. Neurobiol Dis. 2010;38(2):210–8.
10. Van Coevorden-Hameete MH, van Beuningen SFB, Perrenoud M, Will LM, Hulsenboom E, Demonet JF, et al. Antibodies to TRIM46 are associated with paraneoplastic neurological syndromes. Ann Clin Transl Neurol. 2017;4(9):680–6.
11. Yaguchi H, Okumura F, Takahashi H, Kano T, Kameda H, Uchigashima M, et al. TRIM67 protein negatively regulates Ras activity through degradation of 80K-H and induces neuritogenesis. J Biol Chem. 2012;287(15):12050–9.
12. Larman HB, Zhao Z, Laserson U, Li MZ, Ciccia A, Gakidis MA, et al. Autoantigen discovery with a synthetic human peptidome. Nat Biotechnol. 2011;29(6):535–41.
13. Hatakeyama S. TRIM family proteins: roles in autophagy, immunity, and carcinogenesis. Trends Biochem Sci. 2017;42(4):297–311.
14. Oke V, Wahren-Herlenius M. The immunobiology of Ro52 (TRIM21) in autoimmunity: a critical review. J Autoimmun. 2012;39(1–2):77–82.
15. Li Y, Chin LS, Weigel C, Li L. Spring a novel RING finger protein that regulates synaptic vesicle exocytosis. J Bio Chem. 2001;276(44):40824–33.
16. Berti C, Messali S, Ballabio A, Reymond A, Meroni G. TRIM9 is specifically expressed in the embryonic and adult nervous system. Mech Dev. 2002;113(2):159–62.
17. Plooster M, Menon S, Winkle CC, Urbina FL, Monkiewicz C, Phend KD, et al. TRIM9-dependent ubiquitination of DCC constrains kinase signaling, exocytosis, and axon branching. Molecular Biology of the Cell. 2017;28(18):2374–85.
18. Winkle CC, Olsen RH, Kim H, Moy SS, Song J, Gupton SL. Trim9 deletion alters the morphogenesis of developing and adult-born hippocampal neurons and impairs spatial learning and memory. J Neurosci. 2016;36(18):4940–58.
19. Graus F, Saiz A, Dalmau J. Antibodies and neuronal autoimmune disorders of the CNS. J Neurol. 2010;257:509–17.
20. Do LD, Chanson E, Desestret V, Joubert B, Ducray F, Brugière S, et al. Characteristics in limbic encephalitis with anti-adenylate kinase 5 autoantibodies. Neurology. 2017;88(6):514–24.

Affiliations

Le Duy Do[1,2,3] · Stephanie L. Gupton[4] · Kunikazu Tanji[5] · Joubert Bastien[1,2,3] · Sabine Brugière[6] · Yohann Couté[6] · Isabelle Quadrio[7] · Veronique Rogemond[1,2,3] · Nicole Fabien[8] · Virginie Desestret[1,2,3] · Jerome Honnorat[1,2,3,9]

[1] French Reference Center for Paraneoplastic Neurological Syndrome, Hospices Civils de Lyon, Hôpital Neurologique, F-69677 Bron, France

[2] Institut NeuroMyoGene INSERM U1217/CNRS UMR 5310, Université de Lyon - Université Claude Bernard Lyon 1, F-69372 Lyon, France

[3] University of Lyon, Université Claude Bernard Lyon 1, Lyon, F-69372 Lyon, France

[4] Department of Cell Biology and Physiology, University of North Carolina, Chapel Hill, NC 27516, USA

[5] Department of Neuropathology, Institute of Brain Science, Hirosaki University Graduate School of Medicine, 5 Zaifu-cho, Hirosaki 036-8562, Japan

[6] University Grenoble Alpes, CEA, Inserm, BIG-BGE, 38000 Grenoble, France

[7] Neurochemistry Unit, Biochemistry Department, Hospices Civils de Lyon, Groupement Hospitalier Est, Bron, France

[8] Immunology department, Lyon-Sud Hospital, Hospices Civils de Lyon, Pierre-Bénite, France

[9] Neuro-Oncologie, Hôpital Neurologique Pierre Wertheimer, 59 Boulevard Pinel, 69677 Bron Cedex, France